



HAL
open science

A comparison between models for the study of static and dynamic behavior of heterogeneous multilayer composite plates

Alexis Castel, Alexandre Loredo, A. El Hafidi

► **To cite this version:**

Alexis Castel, Alexandre Loredo, A. El Hafidi. A comparison between models for the study of static and dynamic behavior of heterogeneous multilayer composite plates. 2013. hal-00849758

HAL Id: hal-00849758

<https://hal.science/hal-00849758>

Preprint submitted on 31 Jul 2013

HAL is a multi-disciplinary open access archive for the deposit and dissemination of scientific research documents, whether they are published or not. The documents may come from teaching and research institutions in France or abroad, or from public or private research centers.

L'archive ouverte pluridisciplinaire **HAL**, est destinée au dépôt et à la diffusion de documents scientifiques de niveau recherche, publiés ou non, émanant des établissements d'enseignement et de recherche français ou étrangers, des laboratoires publics ou privés.

A comparison between models for the study of static and dynamic behavior of heterogeneous multilayer composite plates

A. Castel^{a,*}, A. Loredo^a, A. El Hafidi^a

^a*DRIVE, Université de Bourgogne, 49 rue Mlle Bourgeois, 58027 Nevers, France*

Abstract

In composite plate structures, it is common to combine different materials with very different Young's moduli and densities. Damping treatments can also be added to prevent high levels of vibration. For discretized problems, the static and dynamic behavior of such heterogeneous structures can be carried out with the 3D elasticity theory but this often leads to very large systems. Therefore, plate theories and particularly equivalent single layer models are often preferred. Classical plate theories have then been adapted to these particular structures using shear correction factors. Higher order shear deformation theories, and more recently transverse shear warping functions, have been proposed. In this work, a model, in which the shear variations through the thickness are described by means of warping functions, is presented. It can handle warping functions proposed by different authors and also the classical theories (Love-Kirchhoff, Mindlin-Reissner and Reddy). To illustrate the behavior of these theories, two studies are presented:

- A sandwich structure with a varying young modulus ratio between the layers is studied using Navier's procedure. Static deflection, shear stress variation through the thickness, and natural frequencies are presented.
- A composite plate covered over 40% of its surface with a constrained layer damping patch is studied. Mean square velocity is computed and compared over a frequency range.

Results are also compared with 3D finite element computations.

Keywords: Multilayered plate model, laminate, vibration

1. Introduction

The mathematical description of the mechanical behavior of plates has been a challenge since the end of the 19th century. Several models describing the behavior of thick and thin plates, like the Love-Kirchhoff and Mindlin-Reissner models, have been developed and are still used up to this day. The study of anisotropic materials and multilayered plates led to adaptations of the two aforementioned models, respectively giving the Classical Lamination Theory (CLT) and the First-order Shear Deformation Theory (FSDT). To improve the way transverse shears are factored into the plate behavior, higher order models have been proposed. Reddy has proposed a third order shear deformation theory often referred as Higher-order Shear Deformation Theory (HSDT). On a different approach, the multilayer structures have been studied by means of models for which the number of unknowns depends on the number of layers, called layer-wise models. However, multilayer structures can also be studied by Equivalent Single Layer (ESL) models like those proposed by Leknitskii, Ambartsumyan, and others.

More recently, some unified formulations of plate models have been proposed (Carrera [1], Demasi [2]) and involve a polynomial description of variables over the third direction. On the other hand, models working with warping functions that take into account transverse shear variations through the thickness have been proposed

*Corresponding author

Email addresses: alexis.castel@u-bourgogne.fr (A. Castel), alexandre.loredo@u-bourgogne.fr (A. Loredo), ali.el-hafidi@u-bourgogne.fr (A. El Hafidi)

(Pai [3], Cho [4], Loredo [5]). These warping functions are not necessarily polynomial and are able to manage complex variations of the shear variation without multiplying the number of variables. Moreover, these functions can be arranged in a manner so it is possible to simulate most of the classical plate theories with the same formulation, leading to a generic ESL model.

In this work, a generic plate model allowing the use of any warping functions for the description of transverse shear stresses is described. Several plate models issued from the literature, including the classical theories, are presented, expressed in terms of warping functions, and compared to each other. First, solutions obtained using Navier's procedure are used to compare the different models with each other and to an analytical solution. Then, the generic plate model is used to evaluate the frequency response of a composite plate partially covered with a Passive Constrained Layer Damping (PCLD) patch. For this case, the excitation is an acoustic plane wave and the comparison is done in terms of mean square velocity for the different models.

2. Generic plate model formulation

In this paper, a generic plate model based on the use of transverse shear warping functions is implemented. It allows the simulation of multilayer laminates made of orthotropic plies using various plate models. Indeed, equivalent single layer (ESL) plate models of the literature can often be formulated in terms of warping functions. As the formulation of this generic model is independent of the choice of the warping functions, it allows the comparison of different models. The generic model is fully described in [5]; we recall here the main components.

2.1. Laminate definition

The laminate is composed of N layers. In this study, all the quantities will be related to those of the middle plane¹; they are marked with the superscript 0. Figure 1 helps to visualize the following definitions:

- z^ℓ is the elevation/offsetting of the middle plane of the layer ℓ
- the ℓ th layer is located between elevations $\zeta^{\ell-1}$ and ζ^ℓ

With these definitions:

- there are N parameters z^ℓ ,
- there are $N + 1$ parameters ζ^i with i taking values from 0 to N ,
- the thickness of the layer ℓ is $h^\ell = \zeta^\ell - \zeta^{\ell-1}$

2.2. Kinematic and static assumptions of the model

In the following, Greek subscripts take values 1 or 2 and Latin subscripts take values 1, 2 or 3. The Einstein's summation convention is used for subscripts only. The comma used as a subscript index means the partial derivative with respect to the following index(ices).

2.2.1. Displacement field

The kinematic assumptions of the present generic model are:

$$\begin{cases} u_\alpha(x, y, z) = u_\alpha^0(x, y) - zw_{,\alpha}^0(x, y) + \varphi_{\alpha\beta}(z)\gamma_{\beta 3}^0(x, y) & (1a) \\ u_3(x, y, z) = w^0(x, y) & (1b) \end{cases}$$

where $u_\alpha^0(x, y)$, $w^0(x, y)$ and $\gamma_{\alpha 3}^0(x, y)$, are respectively the in-plane displacements, the deflection, and the engineering transverse shear strains evaluated at the reference plane. The $\varphi_{\alpha\beta}(z)$ are the four warping functions. The associated strain field is derived from equation (1):

$$\begin{cases} \varepsilon_{\alpha\beta}(x, y, z) = \varepsilon_{\alpha\beta}^0(x, y) - zw_{,\alpha\beta}^0(x, y) + \frac{1}{2} (\varphi_{\alpha\gamma}(z)\gamma_{\gamma 3,\beta}^0(x, y) + \varphi_{\beta\gamma}(z)\gamma_{\gamma 3,\alpha}^0(x, y)) & (2a) \\ \varepsilon_{\alpha 3}(x, y, z) = \frac{1}{2}\varphi'_{\alpha\beta}(z)\gamma_{\beta 3}^0(x, y) & (2b) \\ \varepsilon_{33}(x, y, z) = 0 & (2c) \end{cases}$$

¹The reference plane can be arbitrarily chosen in the laminate assuming that the corresponding transverse shear warping functions are adapted in consequence.

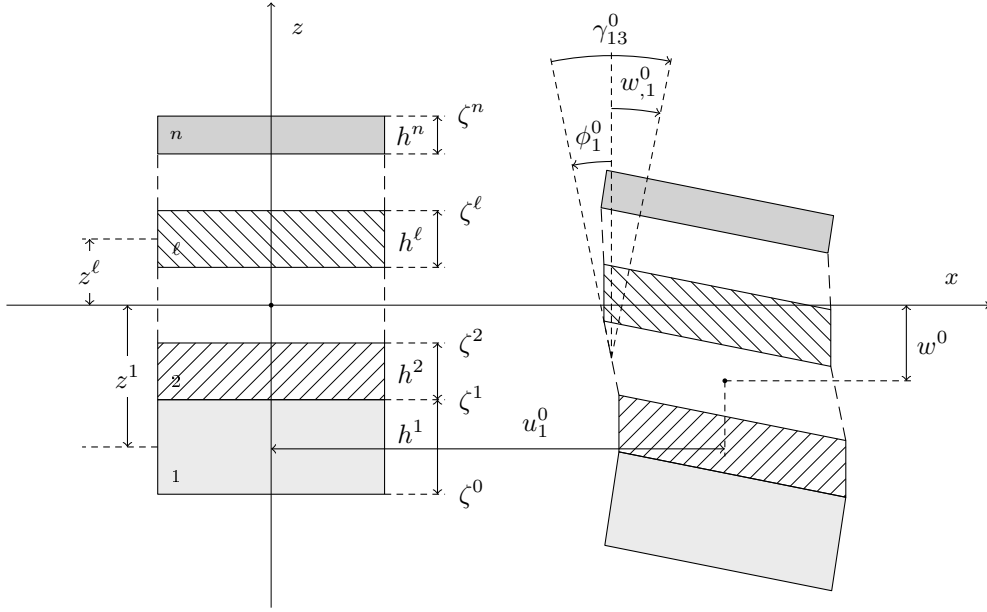


Figure 1: Geometrical parameters of the laminate

which, with the use of Hooke's law, leads to the following stress field:

$$\begin{cases} \sigma_{\alpha\beta}(x, y, z) = Q_{\alpha\beta\gamma\delta}(z) (\varepsilon_{\gamma\delta}^0(x, y) - zw_{,\gamma\delta}^0(x, y) + \varphi_{\gamma\mu}(z)\gamma_{\mu 3,\delta}^0(x, y)) & (3a) \\ \sigma_{\alpha 3}(x, y, z) = C_{\alpha 3\beta 3}\varphi'_{\beta\mu}(z)\gamma_{\mu 3}^0(x, y) & (3b) \\ \sigma_{33}(x, y, z) = 0 & (3c) \end{cases}$$

2.2.2. Static laminate behavior

The model requires introduction of generalized forces:

$$\begin{cases} \{N_{\alpha\beta}, M_{\alpha\beta}, P_{\gamma\beta}\} = \int_{\zeta^0}^{\zeta^n} \{1, z, \varphi_{\alpha\gamma}(z)\} \sigma_{\alpha\beta}(z) dz & (4a) \\ Q_{\beta} = \int_{\zeta^0}^{\zeta^n} \varphi'_{\alpha\beta}(z) \sigma_{\alpha 3}(z) dz & (4b) \end{cases}$$

They are then set, by type, into vectors:

$$\mathbf{N} = \begin{Bmatrix} N_{11} \\ N_{22} \\ N_{12} \end{Bmatrix} \quad \mathbf{M} = \begin{Bmatrix} M_{11} \\ M_{22} \\ M_{12} \end{Bmatrix} \quad \mathbf{P} = \begin{Bmatrix} P_{11} \\ P_{22} \\ P_{12} \\ P_{21} \end{Bmatrix} \quad \mathbf{Q} = \begin{Bmatrix} Q_1 \\ Q_2 \end{Bmatrix} \quad (5)$$

and the same is done for the corresponding generalized strains:

$$\boldsymbol{\epsilon} = \begin{Bmatrix} \epsilon_{11}^0 \\ \epsilon_{22}^0 \\ 2\epsilon_{12}^0 \end{Bmatrix} \quad \boldsymbol{\kappa} = \begin{Bmatrix} -w_{,11}^0 \\ -w_{,22}^0 \\ -2w_{,12}^0 \end{Bmatrix} \quad \boldsymbol{\Gamma} = \begin{Bmatrix} \gamma_{13,1}^0 \\ \gamma_{23,2}^0 \\ \gamma_{13,2}^0 \\ \gamma_{23,1}^0 \end{Bmatrix} \quad \boldsymbol{\gamma} = \begin{Bmatrix} \gamma_{13}^0 \\ \gamma_{23}^0 \end{Bmatrix} \quad (6)$$

Generalized forces are linked with the generalized strains by the 10×10 and 2×2 following stiffness matrices:

$$\begin{Bmatrix} \mathbf{N} \\ \mathbf{M} \\ \mathbf{P} \end{Bmatrix} = \begin{bmatrix} \mathbf{A} & \mathbf{B} & \mathbf{E} \\ \mathbf{B} & \mathbf{D} & \mathbf{F} \\ \mathbf{E}^T & \mathbf{F}^T & \mathbf{G} \end{bmatrix} \begin{Bmatrix} \boldsymbol{\epsilon} \\ \boldsymbol{\kappa} \\ \boldsymbol{\Gamma} \end{Bmatrix} \quad \{\mathbf{Q}\} = [\mathbf{H}] \{\boldsymbol{\gamma}\} \quad (7)$$

with the following definitions of 55 generalized stiffnesses:

$$\left\{ \begin{aligned} \{A_{\alpha\beta\gamma\delta}, B_{\alpha\beta\gamma\delta}, D_{\alpha\beta\gamma\delta}, E_{\alpha\beta\mu\delta}, F_{\alpha\beta\mu\delta}, G_{\nu\beta\mu\delta}\} &= \int_{\zeta^0}^{\zeta^n} Q_{\alpha\beta\gamma\delta} \{1, z, z^2, \varphi_{\gamma\mu}(z), z\varphi_{\gamma\mu}(z), \varphi_{\alpha\nu}(z)\varphi_{\gamma\mu}(z)\} dz & (8a) \\ H_{\alpha 3\beta 3} &= \int_{\zeta^0}^{\zeta^n} \varphi'_{\gamma\alpha}(z) C_{\gamma 3\delta 3} \varphi'_{\delta\beta}(z) dz & (8b) \end{aligned} \right.$$

2.2.3. Laminate equations of motion

Weighted integration of equilibrium equations leads to

$$\begin{cases} N_{\alpha\beta,\beta} = R\ddot{u}_\alpha^0 - S\ddot{w}_{,\alpha}^0 + U_{\alpha\beta}\ddot{\gamma}_{\beta 3}^0 & (9a) \\ M_{\alpha\beta,\beta\alpha} + q = R\ddot{w}^0 + S\ddot{u}_{\alpha,\alpha}^0 - T\ddot{w}_{,\alpha\alpha}^0 + V_{\alpha\beta}\ddot{\gamma}_{\beta 3,\alpha}^0 & (9b) \\ P_{\alpha\beta,\beta} - Q_\alpha = U_{\beta\alpha}\ddot{u}_\beta^0 - V_{\beta\alpha}\ddot{w}_{,\beta}^0 + W_{\alpha\beta}\ddot{\gamma}_{\beta 3}^0 & (9c) \end{cases}$$

with the following definitions of 14 generalized masses,

$$\{R, S, T, U_{\alpha\beta}, V_{\alpha\beta}, W_{\alpha\beta}\} = \int_{\zeta^0}^{\zeta^n} \rho(z) \{1, z, z^2, \varphi_{\alpha\beta}(z), \varphi_{\alpha\beta}(z)z, \varphi_{\mu\alpha}(z)\varphi_{\mu\beta}(z)\} dz \quad (10)$$

and $q = [\sigma_{33}(z)]_{\zeta^0}^{\zeta^n}$ is the value of the transverse loading (no tangential forces are applied on the top and bottom of the plate).

3. Implemented models

All models in this section are implemented with the displacement field described in section 2.2 and will only differ by the chosen set of transverse shear warping functions.

Setting $z = 0$ in equation (1a) and (2b) leads to the following conditions:

$$\begin{cases} \varphi'_{\alpha\beta}(0) = \delta_{\alpha\beta}^K & (11a) \\ \varphi_{\alpha\beta}(0) = 0 & (11b) \end{cases}$$

where $\delta_{\alpha\beta}^K$ is the Kronecker delta.

3.1. Love-Kirchhoff - Classical Lamination Theory

The Classical Lamination Theory (CLT) assumes that straight lines normal to the mid-surface remain straight and normal after deformation, which implies that the transverse shear strains are null. Hence, the angles of rotation of normals are equal to the derivatives of the transverse displacement with respect to x and y . Directions x and y are fully decoupled in the kinematic field. The transverse strain field of the CLT is:

$$\varepsilon_{\alpha 3}(x, y, z) = 0 \quad (12)$$

therefore, equation (2b) permits to identify the $\varphi'_{\alpha\beta}$, which are then integrated according to (11b), so:

$$\begin{cases} \varphi'_{\alpha\beta}(z) = 0 & (13a) \\ \varphi_{\alpha\beta}(z) = 0 & (13b) \end{cases}$$

The **E**, **F**, **G**, and **H** blocks of stiffnesses matrices of equation (7) are null. The system (9) also simplifies to give the classical CLT equations of motion.

3.2. Mindlin-Reissner - First order Shear Deformation Theory

The First Shear Deformation Theory (FSDT) assumes that the transverse shear strains are constant over the thickness of the plate and directions x and y are fully decoupled in the kinematic field. The transverse strain field of the FSDT is

$$\varepsilon_{\alpha 3}(x, y, z) = \frac{1}{2}\gamma_{\alpha 3}^0(x, y) \quad (14)$$

therefore, equation (2b) permits to identify the $\varphi'_{\alpha\beta}$, which are then integrated according to (11b), so:

$$\begin{cases} \varphi'_{\alpha\beta}(z) = \delta_{\alpha\beta}^K & (15a) \\ \varphi_{\alpha\beta}(z) = \delta_{\alpha\beta}^K z & (15b) \end{cases}$$

The **E**, **F**, and **G** blocks respectively contain terms of the **B**, **D**, and **D** blocks, and **H** block is the classical FSDT shear matrix, which can be enhanced by shear correction factors, as it is often done. If we consider the rotation angles $\phi_{\alpha}^0 = -w'_{,\alpha} + \gamma_{\alpha 3}^0$ and the quantities $\psi_{\alpha\beta}^0 = 1/2(\phi_{\alpha,\beta}^0 + \phi_{\beta,\alpha}^0)$ instead of $\kappa_{\alpha\beta}$, equations (7) and (9) can be reformulated to give the classical FSDT stiffness matrices and motion equations.

3.3. Higher-order Shear Deformation Theory or Third-order Shear Deformation Theory

In the Higher-order Shear Deformation Theory (HSDT), first introduced by Reddy [6], the membrane displacements u_{α} are supposed to have a third order variation with respect to z . The shape of the variation has been chosen so that the transverse shear stresses (and then corresponding strains) are null at the plate top and bottom surfaces. The generic model becomes Reddy's model if one takes:

$$\begin{cases} \varphi'_{\alpha\beta}(z) = \delta_{\alpha\beta}^K(1 - \frac{4z^2}{h^2}) & (16a) \\ \varphi_{\alpha\beta}(z) = \delta_{\alpha\beta}^K(z - \frac{4z^3}{3h^2}) & (16b) \end{cases}$$

Note that these functions also verify conditions (11). The first matrix of system (7) can be reduced to a 9×9 matrix because the symmetry of $\varphi_{\alpha\beta}$ permits to combine $\gamma_{13,2}$ and $\gamma_{23,1}$ in a single unknown $1/2(\gamma_{13,2} + \gamma_{23,1})$ denoted κ_6^2 in reference [6] (a similar contraction is done on P_{12} and P_{21}).

3.4. Sun & Whitney (SW)

This model takes into account the multilayer nature of laminates in the kinematic field. It was first described in [7], used for vibroacoustic studies in [8, 9] and extended to off-axis orthotropic plies in [10]. In these works, the kinematic field was not explicitly given, so it was difficult to see the place of this model among plate theories. It has been reformulated into a plate model for static and dynamic studies in [5]. The model requires the continuity of in-plane displacements and transverse shear stresses at each of the $N - 1$ interfaces:

$$\begin{cases} u_{\alpha}^{\ell}(x, y, \zeta^{\ell}) = u_{\alpha}^{\ell+1}(x, y, \zeta^{\ell}) & (17a) \\ \sigma_{\alpha 3}^{\ell}(x, y, \zeta^{\ell}) = \sigma_{\alpha 3}^{\ell+1}(x, y, \zeta^{\ell}) & (17b) \end{cases}$$

where u_{α}^{ℓ} and $\sigma_{\alpha 3}^{\ell}$ are respectively the in-plane displacements and transverse shear stresses in-layer ℓ . In addition, within each layer, the transverse shear strains (and then corresponding stresses) are supposed to have a constant value. This leads to a constant value for each transverse stress $\sigma_{\alpha 3}$ over all the thickness of the plate, assumption which is efficient for sandwiches or PCLD treatments as it can be seen in the results of this study.

The SW conditions added to the general conditions of equation (11) are fulfilled by piecewise linear warping functions and can be written:

$$\begin{cases} \varphi'_{\alpha\beta}(z) = 4S_{\alpha 3\gamma 3}(z)C_{\gamma 3\beta 3}(0) & (18a) \\ \varphi_{\alpha\beta}(z) = 4C_{\gamma 3\beta 3}(0) \int_0^z S_{\alpha 3\gamma 3}(\zeta)d\zeta & (18b) \end{cases}$$

Precautions must be taken with this formula in the case where the reference plane $z = 0$ coincides with an interface. This model needs the full capacity of the generic model, i. e., the 10×10 and 2×2 stiffness matrices of (7) and the complete set of motion equations (9).

3.5. Efficient High Order Plate Theory

This model, introduced in references [4, 11], prescribes, like the SW model, continuity conditions on in-plane displacements and transverse shear stresses at the interfaces but also null transverse stresses at the plate top and bottom surfaces:

$$\begin{cases} \lim_{z \rightarrow \zeta^\ell -} u_\alpha(x, y, z) = \lim_{z \rightarrow \zeta^\ell +} u_\alpha(x, y, z) & (19a) \\ \lim_{z \rightarrow \zeta^\ell -} \sigma_{\alpha 3}(x, y, z) = \lim_{z \rightarrow \zeta^\ell +} \sigma_{\alpha 3}(x, y, z) & (19b) \\ \sigma_{\alpha 3}(x, y, -\frac{h}{2}) = 0 & (19c) \\ \sigma_{\alpha 3}(x, y, +\frac{h}{2}) = 0 & (19d) \end{cases}$$

These conditions are satisfied by the choice of a displacement field, which results in the superposition of cubic polynomials and a zig-zag linear functions of z for the warping functions. It may be written:

$$\begin{cases} \varphi'_{\alpha\beta}(z) = a_{\alpha\beta}z^2 + b_{\alpha\beta}z + c_{\alpha\beta}^\ell & (20a) \\ \varphi_{\alpha\beta}(z) = a_{\alpha\beta}z^3/3 + b_{\alpha\beta}z^2/2 + c_{\alpha\beta}^\ell z & (20b) \end{cases}$$

With the conditions (11), there are now $4N+8$ equations for $4N+8$ unknowns. Thus, the system is solved giving the expected warping functions.

4. Solving processes

Two solving methods are used:

- Navier's procedure for all cross ply laminates;
- Rayleigh-Ritz method for angle ply laminates.

Calculations for cross-ply laminates are compared to exact 3D analytical solutions, and calculations for angle-ply laminates are compared to 3D finite element computations.

4.1. Navier's procedure

This procedure is suitable for (specific) simply supported boundary conditions and for laminates with in-axis orthotropic plies. Each model is implemented in order to simulate the static and dynamic behavior of a square plate with boundary conditions $w = 0$ on the four sides, $u_1 = 0$ on the $y = 0$ and $y = a$ sides and $u_2 = 0$ on the $x = 0$ and $x = a$ sides. The load q is assumed to be a bi-sine function $q(x, y) = \sin(m\pi x/a) \sin(n\pi y/a)$. If more general loads are used, a decomposition of the load with respect to a bi-sine basis can be performed, leading to systems of growing size. However, without loss of generality, the method presented here is for a single order term. With these assumptions, the generalized displacement field is:

$$\begin{pmatrix} u_1 \\ u_2 \\ w \\ \gamma_{13} \\ \gamma_{23} \end{pmatrix} = \begin{pmatrix} u_1^{mn} \cos(m\pi x/a) \sin(n\pi y/a) \\ u_2^{mn} \sin(m\pi x/a) \cos(n\pi y/a) \\ w^{mn} \sin(m\pi x/a) \sin(n\pi y/a) \\ \gamma_{13}^{mn} \cos(m\pi x/a) \sin(n\pi y/a) \\ \gamma_{23}^{mn} \sin(m\pi x/a) \cos(n\pi y/a) \end{pmatrix} \quad (21)$$

where m and n are set to 1 for static analysis, or set to arbitrary chosen values for the dynamic study of the corresponding mode. Then for a given m and n , and for each model, the motion equations 9 give a stiffness and a mass matrix, respectively $[\mathbf{K}]$ and $[\mathbf{M}]$, related to the vector $\{\mathbf{U}\} = \{u_1^{mn}, u_2^{mn}, w^{mn}, \gamma_{13}^{mn}, \gamma_{23}^{mn}\}$. Static (respectively dynamic) response is obtained solving the linear (respectively eigenvalue) problem.

4.2. Rayleigh-Ritz method

In order to manage various boundary conditions, laminates sequences, and types of loadings, a numerical code based on the Rayleigh-Ritz method, previously described in references [12, 13], has been updated in order to accept off-axis orthotropic plies. This code builds a stiffness matrix $[\mathbf{K}]$ and a mass matrix $[\mathbf{M}]$ from which we can obtain:

- eigenvalues, and then the natural angular frequencies.
- a response to a given load: for this study we will focus on an acoustic progressive plane wave of incidence angles $\varphi = 45^\circ$ and $\theta = 45^\circ$, the definition of those angles is illustrated in figure 2.

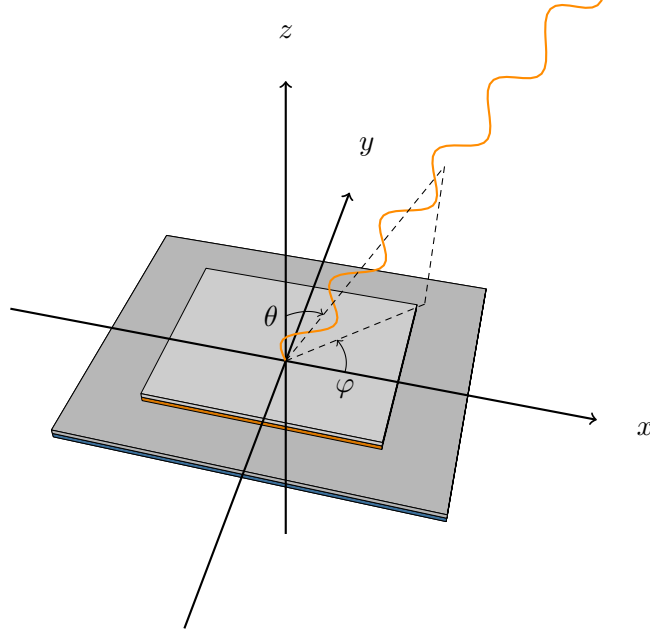


Figure 2: View of a patched plate submitted to an acoustic plane-wave, showing the definition of the angles of incidence φ and θ° .

The basis used for all calculations with the Rayleigh-Ritz code is the enriched trigonometric basis described by Beslin [14]. Results are obtained with a 40×40 basis.

5. Numerical results

5.1. Orthotropic sandwich composite plate

This section aims at studying a squared five layer sandwich panel $[0^\circ/90^\circ/\text{core}/0^\circ/90^\circ]$ with a fixed ratio of thickness core to flange $t_c/t_f = 10$. The face sheets (Graphite-Epoxy) have the following properties:

$$\frac{E_1^f \text{ (GPa)}}{109} \quad \frac{E_2^f = E_3^f \text{ (GPa)}}{8.819} \quad \frac{G_{23}^f}{3.2} \quad \frac{G_{13}^f \text{ (GPa)} = G_{12}^f \text{ (GPa)}}{4.315} \quad \frac{\nu_{23}^f}{0.38} \quad \frac{\nu_{12}^f = \nu_{13}^f}{0.342} \quad \frac{\rho^f \text{ (kg.m}^{-3}\text{)}}{1627} \quad \frac{\eta}{0.05}$$

The core material is made of an isotropic foam that its properties depend on the flange properties E_1^f and a factor a :

$$\frac{E_1^c = E_2^c = E_3^c \text{ (GPa)}}{a \times E_1^f} \quad \frac{G_{12}^c = G_{23}^c = G_{13}^c \text{ (GPa)}}{0.5 \times a \times E_1^f} \quad \frac{\nu_{12}^c = \nu_{13}^c = \nu_{23}^c}{0} \quad \frac{\rho^c \text{ (kg.m}^{-3}\text{)}}{100}$$

Three nondimensionalized parameters will be observed and compared to the results obtained from an analytical solution:

- The static deflection to a sinusoidal pressure. All deflections are nondimensionalized using equation (23), h being the total thickness of the plate, E_2^c the transverse Young’s modulus of the core material.

$$\bar{w} = \frac{100wE_2^c h^3}{l_x^4} \quad (22)$$

- The transverse shear variation through the thickness:

$$\bar{\sigma}_{\alpha 3} = \frac{10h\sigma_{\alpha 3}(z)}{l_x} \quad (23)$$

- The first natural frequency of the plate. All frequencies are nondimensionalized using equation (24); ρ^c and E_2^c are respectively the density and the transverse Young’s modulus of the core material.

$$\bar{\omega} = (\omega l_x^2/h)\sqrt{\rho^c/E_2^c} \quad (24)$$

Note that, due to the symmetry of the panel’s configuration, it is only necessary to present σ_{13} , since σ_{23} is the same as σ_{13} with a symmetry over the reference plane.

Model	a						
	10^0	10^{-1}	10^{-2}	10^{-3}	10^{-4}	10^{-5}	10^{-6}
CLT	0.3475	1.2700	1.7299	1.7950	1.8018	1.8024	1.8025
FSDT	0.4081	1.8104	4.3144	5.9523	6.2285	6.2581	6.2610
HSDT	0.4152	1.8229	6.4263	30.520	61.623	68.900	69.726
SW	0.3713	1.7746	6.8137	50.524	362.66	1007.3	1226.1
EHOPT	0.4152	1.8201	6.8397	50.535	362.53	1007.2	1226.1
Analytical solution	0.4147	1.8462	7.0849	52.215	372.63	1021.7	1238.1

Table 1: Static deflection $\bar{w} = \frac{100wE_2^0 h^3}{l_x^4}$ for the sandwich panel, with $l_x/h = 4$ for different models and for various values of a .

The analytical solution is derived from Pagano’s plate bending solution. The plate loading is equally divided between the top and bottom planes of the sandwich panel. Note that this conflicts with the plane stress condition, especially with high thickness to length ratio and/or with high Young’s modulus ratio between the layers. Therefore, part of the difference, shown in table 1 is explained by this. This explains the result quality improvement of every model when compared to the analytical solution between tables 1 and 2 since there is no loading involved in the fundamental natural frequency calculation.

When looking at tables 1 and 2, as expected, and for both cases, the HSDT gives satisfying results when $a = 10^0$, since the sandwich panel’s foam has a Young’s modulus close to the flanges’ properties. The SW model tends to give better results with lower values of a , and generally, the EHOPT model gives satisfying results for both the static deflection and fundamental frequency, excepted for the case where $a = 10^{-6}$. For this last case, true variation of transverse shear stresses is too far apart from what can be fitted the EHOPT warping functions. Observing transverse shear stresses in figure 3 confirms that none of the present warping functions manage to perfectly fit the analytical solution.

5.2. Patched composite plate

In this section a composite plate damped with a PCLD patch is considered for a dynamic study. The base plate has the following stacking sequence $[0^\circ/45^\circ/90^\circ/-45^\circ]_S$. Every ply is made of 0.15 mm of Graphite-Epoxy (material properties are given in section 5.1). The damping coefficient has been set to 0.05. The patch is made with a viscoelastic layer made of ISD112 and an aluminum constraining layer. Both layers are 0.2 mm thick. The ISD112 Young’s modulus is frequency dependent and is given in table 3. Other properties include $\nu_{12} = \nu_{13} = \nu_{23} = 0.45$ and $\rho = 1015 \text{ kg.m}^{-3}$. The aluminum alloy has Young’s modulus of 72.4 GPa, Poisson’s coefficient of 0.33, density of 2780 kg.m^{-3} , and damping coefficient of 0.005.

The studied case belongs to the thin plate category (thickness to length ratio of 0.002); however, the PCLD patch involves a high Young’s modulus ratio between the layers. Since the plate is thin and because they do

Model	a						
	10^0	10^{-1}	10^{-2}	10^{-3}	10^{-4}	10^{-5}	10^{-6}
CLT	32.693	17.241	14.771	14.500	14.472	14.470	14.469
FSDT	31.135	15.108	10.131	8.6721	8.5041	8.4847	8.4827
HSDT	30.862	15.041	8.3819	3.8746	2.7272	2.5792	2.5639
SW	32.422	15.236	8.1469	3.0121	1.1243	0.6746	0.6115
EHOPT	30.825	15.048	8.1316	3.0117	1.1245	0.6746	0.6115
Analytical solution	30.845	14.962	8.0619	2.9843	1.1171	0.6719	0.5753

Table 2: Dimensionless fundamental natural frequency $\bar{\omega} = (\omega a^2/h)\sqrt{\rho/E_a}$ for the sandwich plate, with $l_x/h = 4$ for different models and for various values of a .

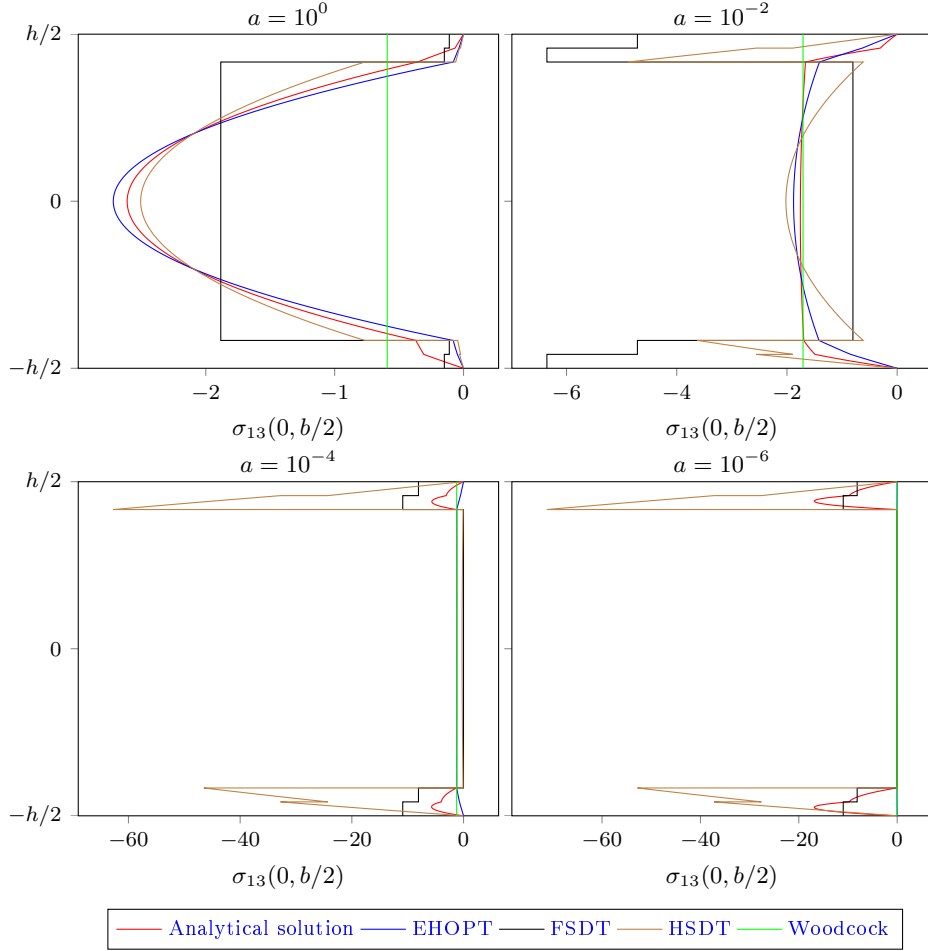


Figure 3: Transverse shear strain repartition

Frequency (Hz)	Young's Modulus (Pa)
10	7.28×10^5
100	2.34×10^6
500	5.20×10^6
1000	7.28×10^6
2000	9.88×10^6
3000	1.17×10^7
4000	1.38×10^7

Table 3: Frequency dependence of the mechanical properties of the viscoelastic material ISD 112 ($T = 25^\circ\text{C}$)

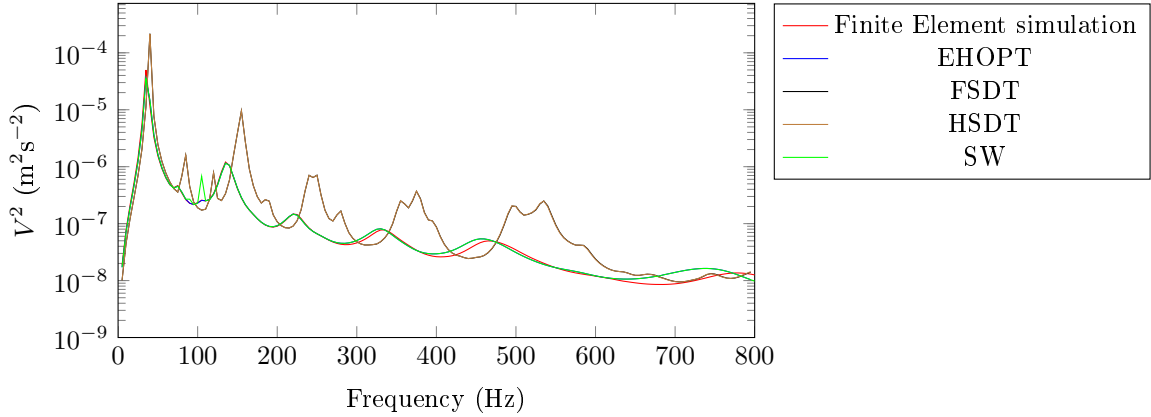


Figure 4: Mean Square Velocity of the patched composite plate for different models and the three dimensional finite element simulation (mesh $25 \times 20 \times 8 + 15 \times 12 \times (4 + 1)$ 20-node hexahedrons).

not take the material properties into account; the FSDT and HSDT give similar results. The other two models (SW and EHOPT) take into account the viscoelastic layer properties. Therefore, they give better results than the other two models. However, as the plate is thin, SW and EHOPT do not differentiate from each other. If a higher length to thickness ratio had been chosen, all models would have probably given different results.

We can notice from figure 4 that the three dimensional finite element results differ from the two better models. This is due to the lack of refinement of the finite element mesh. Indeed, for a simpler configuration with a single layer base plate, a previous study [13] of the same nature has shown that a more refined mesh was necessary to converge up to 800 Hz. Unfortunately, with 8 layers, it is fairly difficult to manage to have converged results in the higher frequency range.

6. Conclusion

A generic plate model has been formulated using warping functions in order to describe the transverse shear stresses. This model can handle classical plate theories as well as more refined models. Using this generic model allowed the comparison of those theories from a static and dynamic point of view. It is shown that improved formulations of warping functions give satisfying results. Transverse shear stresses can be evaluated directly from the kinematic field or by integration of the equilibrium equations. Even with the more refined models that give satisfying results in terms of deflections or natural frequencies, the direct estimation of the transverse shear stresses directly from the kinematic field does not give systematically acceptable results. However, the generic plate model, as it is presented, allows one to propose a new set of functions and easily implement it.

The dynamic study of a composite plate with a damping treatment, for which high Young's modulus ratios between the layer are present, also illustrates the importance of the choice of the model.

References

- [1] E. Carrera. Theories and finite elements for multilayered, anisotropic, composite plates and shells. *Archives of Computational Methods in Engineering*, 9(2):87–140, 2002.

- [2] Luciano Demasi. Mixed plate theories based on the generalized unified formulation.: Part ii: Layerwise theories. *Composite Structures*, 87(1):12 – 22, 2009.
- [3] Perngjin F. Pai. A new look at shear correction factors and warping functions of anisotropic laminates. *International Journal of Solids and Structures*, 32(16):2295–2313, 1995.
- [4] Maenghyo Cho and R. R. Parmerter. Efficient higher order composite plate theory for general lamination configurations. *AIAA Journal*, 31:1299–1306, July 1993.
- [5] A. Loredo and A. Castel. A multilayer anisotropic plate model with warping functions for the study of vibrations reformulated from woodcock’s work. *Journal of Sound and Vibration*, 332(1):102–125, 2013.
- [6] J. N. Reddy. A simple higher-order theory for laminated composite plates. *Journal of Applied Mechanics*, 51(4):745, 1984.
- [7] C.T. Sun and J.M. Whitney. Theories for the dynamic response of laminated plates. *AIAA Journal*, 11(2):178, 1973.
- [8] J. L. Guyader and C. Lesueur. Acoustic transmission through orthotropic multilayered plates, part i :plate vibration modes. *Journal of Sound and Vibration*, 97:51–68, 1978.
- [9] R. L. Woodcock and J. Nicolas. A generalized model for predicting the sound transmission properties of generally orthotropic plates with arbitrary boundary conditions. *The Journal of the Acoustical Society of America*, 97:1099–1112, 1994.
- [10] Roland L. Woodcock. Free vibration of advanced anisotropic multilayered composites with arbitrary boundary conditions. *Journal of Sound and Vibration*, 312(4-5):769–788, may 2008.
- [11] Maenghyo Cho and R.Reid Parmerter. An efficient higher-order plate theory for laminated composites. *Composite Structures*, 20(2):113–123, 1992.
- [12] Alexandre Loredo, Arnaud Plessy, Ali El Hafidi, and Nacer Hamzaoui. Numerical vibroacoustic analysis of plates with constrained-layer damping patches. *The Journal of the Acoustical Society of America*, 129(4):1905–1918, 2011.
- [13] A. Castel, A. Loredo, A. El Hafidi, and B. Martin. Complex power distribution analysis in plates covered with passive constrained layer damping patches. *Journal of Sound and Vibration*, 331(11):2485–2498, May 2012.
- [14] O. Beslin and J. Nicolas. A hierarchical functions set for predicting very high order plate bending modes with any boundary conditions. *Journal of Sound and Vibration*, 202(5):633 – 655, 1997.